Thermodynamic properties and crystallization kinetics of glass-forming undercooled liquid Au-Pb-Sb alloys

H. J. Fecht
Universität Augsburg, Institut für Physik, Memminger Strasse 6, 8900 Augsburg, Federal Republic of Germany

J. H. Perepezko
University of Wisconsin, Department of Materials Science and Engineering, 1509 University Avenue, Madison, Wisconsin 53706

M. C. Lee
NASA Headquarters, Microgravity Science and Applications, Code EN, Washington, DC 20546

W. L. Johnson
W. M. Keck Laboratory of Engineering Materials, California Institute of Technology, 138-78, Pasadena, California 91125

(Received 27 April 1990; accepted for publication 19 June 1990)

The heat capacities of liquid and crystalline Au-Pb-Sb alloys in the glass-forming composition range were measured with droplet emulsion and bulk samples. Based on the measured C_p data, the entropy, enthalpy, and Gibbs free-energy differences between the eutectic solid mixture and undercooled liquid were determined as a function of temperature over $\sim 60\%$ of the undercooling range below the liquidus temperature and compared with theoretical predictions. The results indicate an isentropic temperature at 313 ($\pm$ 5) K, which agrees well with experimental data for the glass transition. The thermodynamic evaluation was applied further to develop a kinetics analysis of the nucleation undercooling response during cooling. Use of different approximations for the Gibbs free energy leads to a variation of the prefactor terms of six orders of magnitude for classical nucleation theory and, consequently, large variation in calculated transformation diagrams which is more pronounced with increasing undercooling. Extrapolations into the glass-forming temperature range and the effects of viscosity, transient nucleation, and estimated Kauzmann temperatures on the crystallization kinetics at high undercooling have been evaluated. This analysis reveals the importance of using measured values of thermophysical properties, even if they represent a limited temperature range at modest undercooling, rather than model approximations in order to obtain reliable evaluations of crystallization kinetics at high undercooling in the glass-forming temperature range.

I. INTRODUCTION

Liquid Au-Pb-Sb alloys can be quenched to a metallic glass at varying cooling rates ranging from 10^6 K/s (splat quenching)[1] to 10^3 K/s (drop tube processing).[2] At the low cooling rates, millimeter size droplets and hollow spheres with amorphous structure have been successfully produced. During cooling below the eutectic temperature, the phase selection for crystallization is determined by competition between nucleation and growth of the different metastable and stable phases. In order to predict the final transformation products which can be amorphous or crystalline, knowledge of the thermodynamic properties of the metastable liquid and solid phases in the undercooled regime becomes necessary. In particular, the entropy and enthalpy differences between the crystalline and undercooled liquid phases are of interest and can be evaluated from available heat capacity data.

Experimentally, deep undercooling levels of a liquid can be attained by a slow cooling of a droplet emulsion.[3] With droplet samples measurements of the heat capacities of undercooled liquid and crystalline solid phases of Au-Pb-Sb alloys in the glass-forming composition range have been made by means of differential scanning calorimetry. This allows determination of the thermodynamic properties of metastable phases including the enthalpies, entropies, and Gibbs free energies of the undercooled liquid. In addition, the kinetics of crystallization from the highly undercooled liquid has been examined. The crystallization kinetics is related to the undercooling and cooling rate based on the experimentally determined Gibbs free energies and is compared with different models that attempt to predict the free-energy difference between the liquid and the stable crystalline state.

II. EXPERIMENTAL APPROACH AND ANALYSIS

Deep undercooling levels of liquid metals below the melting temperature T_m can be reached by the use of the droplet emulsion method[3] under low cooling rate conditions. Basically, the principle of the droplet emulsion technique rests upon the isolation of potential nucleation centers by the dispersion of a given quantity of liquid metal (e.g., 1 g) into a large number of drops (about 10^7). Droplet samples were prepared by shearing a mixture of carrier fluid and liquid alloy (99.99% purity) under an inert atmosphere into

 0021-8979/90/214494-09$03.00 © 1990 American Institute of Physics

Downloaded 12 Jan 2006 to 131.215.240.9. Redistribution subject to AIP license or copyright, see http://jap.aip.org/jap/copyright.jsp

an emulsion with an average diameter of 10 μm. Applying a relatively noncatalytic coating, crystallization can be prevented in a temperature range up to 0.3 to 0.4 T_m on a time scale long enough to allow measurements of characteristic properties of the undercooled liquid. The emulsification approach allows glass formation in droplet samples during slow cooling (10–20 K/min) in a few alloy systems.[4]

The droplet method has been applied to Au-Pb-Sb alloys[5] with a composition range close to the ternary eutectic. This has been demonstrated to be within the glass formation range of Au-Pb-Sb alloys applying cooling rates of about 10^5 K/s.[1] For example, Fig. 1 depicts the x-ray spectrum of a $Au_{55}Pb_{22.5}Sb_{22.5}$ alloy quenched at a rate of 10^5 K/s.

The undercooling, heat capacity, and reaction kinetics were measured with a differential scanning calorimeter, Perkin-Elmer DSC7, under computer control. Reaction temperatures were corrected for instrumental temperature lag. In order to optimize the accuracy of reaction temperature determination, two standard samples were used with sharp melting temperatures that spanned the temperature range of measurement. For this calibration, eutectic signals T_E from a Sn-(20 at. %) Bi alloy ($T_E = 412$ K) and a Au-Pb-Sb bulk sample ($T_E = 523$ K) were used. For heat capacity measurements sapphire was taken as a standard for calibration. To establish good baseline reproducibility during C_p measurements, samples were always subjected to several overlapping scans in a range of 40 K with a scanning rate of 10 K/min.

The heat capacities of the crystalline phase and of the liquid phase in bulk form which could be undercooled by a small amount below the liquidus temperature T_L have been measured with an accuracy of $\pm$ 1%. For the measurement of C_p of the undercooled liquid, droplet samples were used. At low undercooling, droplet samples were utilized with the carrier fluid removed. For C_p measurement at large undercooling, the droplet samples were used as emulsified. Because a small amount of droplets with high catalytic potency crystallized during cooling at low undercooling levels, the heat capacity cannot be accurately measured for droplet samples during a cooling cycle. Therefore, to avoid interference between heat capacity and crystallization effects, C_p for highly undercooled droplet samples was measured during heating cycles and the following procedure was chosen. First, the liquid droplets were cooled from 50 K above the liquidus temperature to a temperature 20 K above the average nucleation temperature with a rate of 20 K/min, which caused a relatively small amount $X(\%)$ of liquid to crystallize in a few droplets with high catalytic potency. Solidification of a metastable crystalline phase which nucleates at maximum undercooling[5] has not been observed in this temperature range. Subsequently, the heat capacity C_p^A of droplet samples containing carrier fluid, liquid alloy, and crystalline phase was measured during several heating scans as the sum given by

$$C_p^A = C_p^{\text{oil}} + (1 - X)C_p^L + XC_p^x, \tag{1a}$$

where C_p^{oil}, C_p^L, and C_p^x represent the heat capacities of carrier fluid, metallic liquid, and crystalline (eutectic) metallic phase, respectively. Then, the sample was crystallized completely and held at room temperature for several minutes which allowed any metastable crystalline phases to decompose completely. In a subsequent heating run, the heat capacity C_p^B of the stable crystalline phases plus carrier fluid was obtained as

$$C_p^B = C_p^{\text{oil}} + C_p^x. \tag{1b}$$

By subtraction of Eqs. (1a) and (1b) the heat capacity difference ΔC_p between the liquid-crystalline mixture and the completely crystallized phase $\Delta C_p = C_p^A - C_p^B$ was calculated. Consequently, the liquid heat capacity was determined as

$$C_p^L = [\Delta C_p + (1 - X)C_p^x]/(1 - X). \tag{2}$$

With this approach the heat capacity of the highly undercooled liquid phase C_p^L is related to the heat capacity C_p^x

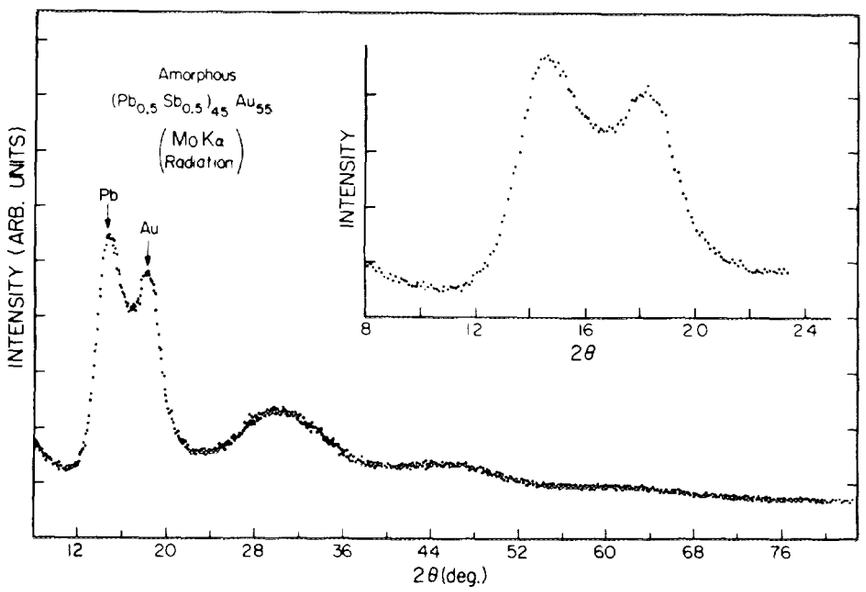

FIG. 1. X-ray spectra of amorphous $Au_{55}Pb_{22.5}Sb_{22.5}$ using MoKα radiation.

Downloaded 12 Jan 2006 to 131.215.240.9. Redistribution subject to AIP license or copyright, see http://jap.aip.org/jap/copyright.jsp

of the crystalline phases measured with the bulk samples. The relative amount X of the crystalline phases was estimated by integration of the melting peak of the partially crystallized sample. The sample mass was estimated by relating the integrated signal of melting to the heat of fusion measured for a bulk sample with the same composition and accurately known mass. Considering the cumulative steps involved in this measurement, the C_p data of the highly undercooled liquid were obtained with an estimated accuracy of $\pm 5\%$.

For evaluation of the nucleation kinetics during crystallization from the highly undercooled liquid, the cooling rate has been varied between 10 and 300 K/min and related to the measured nucleation temperatures taken as the onset of the nucleation exotherm. With the nucleation temperatures corrected for instrumental temperature lag, the reaction kinetics can be analyzed in combination with classical nucleation theory and the experimentally determined Gibbs free energies of the highly undercooled liquid and eutectic solid.

Based on the classical nucleation theory for heterogeneous nucleation the steady-state nucleation rate J_a can be represented as[6,7]

$$J_a = \Omega_a/\eta \exp(-\Delta G^*/k_B T). \tag{3}$$

Appropriate values for the prefactor, Ω_a, and nucleation barrier ΔG^* can be derived for Eq. (3) as has been shown previously for solidification of Hg.[7] The liquid viscosity η is given by[8]

$$\eta(T) = 10^{-3.3} \exp[3.34 T_E/(T - T_{g0})], \tag{3a}$$

with T_{g0} being the ideal glass transition temperature. The activation barrier ΔG^* is given by

$$\Delta G^* = b\sigma_{xL}^3 f(\theta)/\Delta G_V^2, \tag{3b}$$

where σ_{xL} is the crystal/liquid interfacial energy, $f(\theta)$ a function of the contact angle θ where, for example, $f(\theta) = 0.25(2 - 3\cos\theta + \cos^3\theta)$ for spherical nuclei, ΔG_V is the driving free energy for nucleation per unit volume of product phase and equals the Gibbs free energy difference of the liquid and the stable crystalline phase mixture $G^L(T) - G^x(T)$, and $b = 16\pi/3$ is a geometrical factor.

During continuous cooling at low rates the onset of solidification occurring within the time t in a droplet of catalytic surface area, a, with a heterogeneous nucleation rate, J_a, per unit area can be approximated as[9]

$$J_a(T_N)at = K(T_N), \tag{4}$$

where K represents a constant at the nucleation temperature T_N which ranges typically from 100 to 200.

Combining Eqs. (3) and (4) then leads to the relationship

$$\ln t = -\ln\{a\Omega_a/[K(T_N)\eta]\} + b\sigma_{xL}^3 f(\theta)/(\Delta G_V^2 k_B T). \tag{5}$$

Here, t describes the heterogeneous nucleation time for the appearance of the eutectic solid during continuous cooling at rates that allow for the maintenance of steady-state conditions. This allows to determine the prefactor term $A = a\Omega_a/[K(T_N)\eta]$ and the interfacial energy related term $B = b\sigma_{xL}^3 f(\theta)/k_B$ from the experimental results. The dependence on the undercooling level ΔT (temperature difference between the eutectic temperature T_E and nucleation temperature T_N) on the cooling rate $\dot{T}$ is measured by differential scanning calorimetry (DSC) with the time t corresponding to $\Delta T/\dot{T}$. This approach is applied for Au-Pb-Sb alloys which show a well-defined crystallization onset at large undercooling.[5] The application of Eq. (5) to the multicomponent eutectic would certainly involve a more detailed assessment of the energetics of nucleus development than outlined above. For example, the solid-solid interfaces between the eutectic α and β phases, which might have spacings $\leqslant 10^2$ Å, are neglected in the thermodynamic term. For the purpose of the present analysis, however, it is important to note that the main factors that constitute the nucleation barrier will be retained in a more complete analysis. With this in mind, the influence of the use of actual measurements (as compared with estimates of the thermodynamic driving force) on the nucleation kinetics can be evaluated without the uncertainty of the actual nucleus identity.

III. EXPERIMENTAL RESULTS

Using droplet samples a maximum undercooling level of 0.3 T_L below the liquidus temperature T_L was achieved at a cooling rate of 20 K/min, resulting in a single, well-defined crystallization exotherm.[5] The droplet samples were stable enough to sustain several heating and cooling cycles without a change in the undercooling characteristics. The composition closest to the ternary eutectic composition and still in the glass-forming range[1] was found as $Au_{53.2}Pb_{27.5}Sb_{19.3}$ with the eutectic temperature T_E at 523 K and T_L at 573 K. It can be noted that the liquidus slope for this alloy is quite steep, which is a common characteristic of easy glass-forming eutectic alloys. The maximum undercooling temperature for dispersed droplet samples at a cooling rate of 20 K/min was found as 398 K, which corresponds to an undercooling level of 175 K below T_L. The heat of fusion ΔH_f of a eutectic crystalline mixture at T_E was obtained by DSC measurements at a heating rate of 20 K/min to be 8.25 kJ/mol with a corresponding entropy of fusion ΔS_f of 15.78 J/mol K.

For the measurement of the liquid heat capacity at temperatures above T_L, bulk samples have been used. This allowed the determination of the liquid heat capacity C_p^L between 570 and 670 K. The heat capacity of the undercooled liquid has been measured between 423 and 570 K using droplet samples. By cooling the emulsified droplet samples at 20 K/min below the eutectic temperature to 423 K, about $X = 10\%$ of the droplet population (with high catalytic potency of the nucleation sites) crystallized to the stable eutectic phase, whereas 90% remained liquid until the maximum undercooling temperature was reached.

The obtained heat capacity data of bulk and droplet samples are shown in Fig. 2. The liquid heat capacity C_p^L is seen to decrease with increasing temperature and goes smoothly through the liquidus temperature T_L connecting the bulk and droplet sample values. The measured C_p^L values for the highly undercooled liquid rise to high values when approaching the eutectic temperature T_E probably due to nonequilibrium effects during melting of the small crystalline part of the sample and have not been included in the figure. The C_p values for the liquid are fitted numerically by

Downloaded 12 Jan 2006 to 131.215.240.9. Redistribution subject to AIP license or copyright, see http://jap.aip.org/jap/copyright.jsp

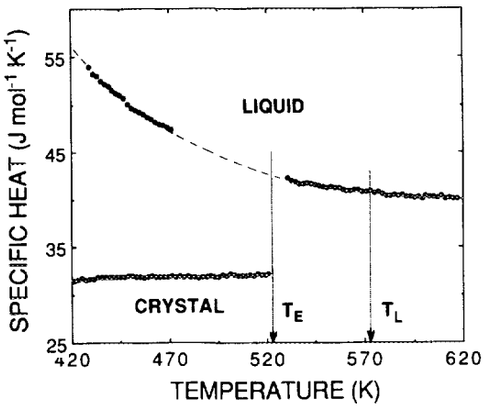

FIG. 2. Heat capacity data measured for liquid and crystalline $Au_{53.2}Pb_{27.5}Sb_{19.3}$ alloys.

the following equation: $C_p^L = -47.4 + 9.4\times10^{-2}\,T + 1.11\times10^{7}\,T^{-2}$ J/mol K, whereas for the crystalline solid a linear approximation was sufficient with $C_p^x = 29.1 + 5.9\times10^{-3}\,T$ J/mol K. It is interesting to note here that the heat capacity difference between the crystalline and liquid phase at the eutectic temperature (about 10 J/mol K) is rather large if compared to pure metals at the melting point. Pure metals have heat capacities that are equal within 100 K of the melting temperature.[15] This feature of Au-Pb-Sb alloys is important in terms of the glass-forming ability which is usually estimated in terms of the reduced glass transition temperature as discussed below.

Consequently, the measured heat capacity data can be used to calculate the thermodynamic properties of the undercooled liquid L and eutectic crystalline solid x (the eutectic mixture is treated as one solid) below the eutectic temperature T_E. The entropy $S(T)$ of liquid phase L and crystalline phase x is described as a function of temperature as

$$S^L(T) = \Delta S_f + \int_{T_E}^{T} C_p^L/T\,dT, \tag{6a}$$

$$S^x(T) = \int_{T_E}^{T} C_p^x/T\,dT. \tag{6b}$$

The entropies of the metastable liquid, S^L, and of the eutectic solid, S^x, are represented in Fig. 3 as function of temperature. The entropy of the undercooled liquid decreases faster than the entropy of the stable crystalline phase if the temperature is reduced. If the entropy values are extrapolated beyond the experimentally determined range which is indicated by the dashed line in Fig. 3, a temperature is obtained at which the entropies of undercooled liquid and crystalline solid become equal. This isentropic temperature $T_{\Delta S=0}$ is found to be 313 K.

The enthalpies H^L and H^x are calculated based on the same C_p extrapolations for the heat capacities as

$$H^L(T) = \Delta H_f + \int_{T_E}^{T} C_p^L\,dT, \tag{7a}$$

$$H^x(T) = \int_{T_E}^{T} C_p^x\,dT, \tag{7b}$$

and are shown in Fig. 4. Extrapolating the enthalpy values beyond the measured temperature range, i.e., extending the curve for the undercooled liquid below the crystallization temperature, it is seen from Fig. 4 that solidification under adiabatic conditions[10] becomes possible below the temperature $T_h = 365$ K. This temperature marks the start of the hypercooled regime where the enthalpy of the undercooled liquid $H^L(T_h)$ equals the enthalpy of the eutectic solid $H^L(T_E)$ at the eutectic temperature and is only about 35 K below the average nucleation temperature in the droplet population at a cooling rate of 20 K/min.

Based on Eqs. (6a) and (6b) and (7a) and (7b) the Gibbs free energies of undercooled liquid and eutectic solid are obtained as

$$G^L(T) = H^L(T) - TS^L(T), \tag{8a}$$

$$G^x(T) = H^x(T) - TS^x(T), \tag{8b}$$

and are shown in Fig. 5. The isentropic temperature $T_{\Delta S\ 0}$

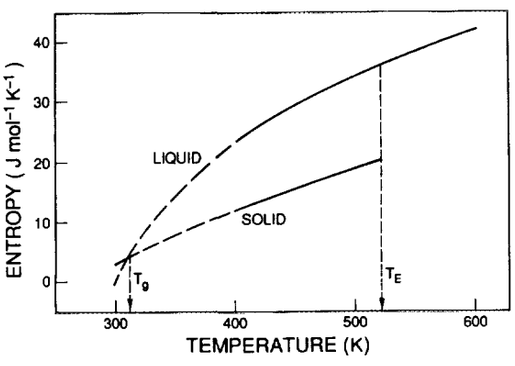

FIG. 3. Entropies of undercooled liquid and eutectic solid based on measured (solid line) and extrapolated (dashed line) C_p data. An isentropic temperature T_{s0} is obtained as 313 K ($\pm$ 5 K) which corresponds to the ideal glass transition temperature.

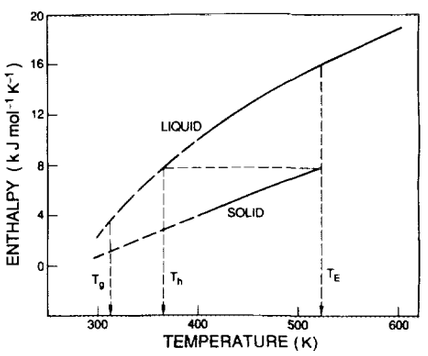

FIG. 4. Enthalpies of undercooled liquid and eutectic solid based on measured (solid line) and extrapolated (dashed line) C_p data. Conditions for adiabatic solidification are obtained below $T_h = 365$ K.

Downloaded 12 Jan 2006 to 131.215.240.9. Redistribution subject to AIP license or copyright, see http://jap.aip.org/jap/copyright.jsp

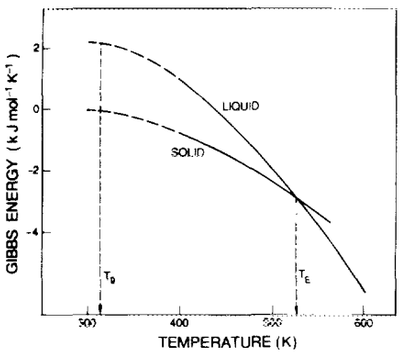

FIG. 5. Gibbs free energies of undercooled liquid and eutectic solid based on measured (solid line) and extrapolated (dashed line) C_p data.

where the entropies of both phases become equal is characterized in the free-energy curves by the parallel slope $\partial G^x/\partial T = \partial G^L/\partial T$ in both curves.

In addition to the determination of the thermodynamic properties in the metastable regime, the droplet samples which solidify at maximum undercooling in one single reaction have also been used for determination of the nucleation kinetics. Based on the theory as outlined above, the cooling rate results are plotted in Fig. 6 in terms of Eq. (5) as $\ln t$ vs $(\Delta G_v^2 T)^{-1}$ for a sample which solidified at 424.6 K at a cooling rate of 20 K/min, i.e., still in the temperature range of the experimentally determined Gibbs free energies [Eqs. (8a) and (8b)]. For these samples, the nucleation temperature decreased from 425.2 to 419.9 K if the cooling rate was varied from 10 to 300 K/min with the nucleation temperatures obtained at the highest cooling rates (short times) being less accurate than those obtained at the low cooling rates. In Fig. 6 the time t is given by $\Delta T/\dot{T}$, and ΔG_v is based on the experimentally determined heat capacity data. The kinetics measurements are fitted to Eq. (5) which can be written as

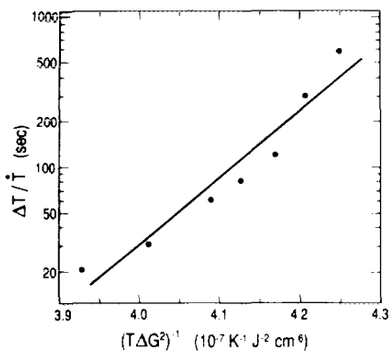

FIG. 6. Nucleation kinetics plot based on continuous cooling measurements for $Au_{53.2}Pb_{27.5}Sb_{19.3}$ droplets.

$\ln t = -\ln A + B/\Delta G_v^2 T$ with a value of $A = 1.8\times10^{16}$ s^{-1} and a slope $B = 1.02\times10^8$ K J^2 cm^{-6} as obtained by a least-square fit. From the obtained value for B, an activation energy per atom for nucleation of the crystalline phase is calculated as $\Delta G^* = Bk_B/\Delta G_v^2$, which corresponds to 1.5 eV/atom.

IV. DISCUSSION

Heat capacity measurements of the undercooled liquid of a glass-forming alloy using droplet samples are presented here covering a much wider temperature range than previous measurements.[11,12] In accord with other heat capacity measurements for undercooled liquids, which have been done for pure metals[13] and glass-forming alloys in a smaller temperature range,[11,12] the heat capacity of the undercooled liquid rises with decreasing temperature. This effect is much more pronounced for glass-forming alloys like Au-Pb-Sb than for pure metals, e.g., Hg, Sn, Bi, In,[13] and has important consequences for the thermodynamic properties of the undercooled liquid and evaluation of crystallization kinetics.

One of the main parameters which describes the ability of an alloy system to form a glass is based on the entropy difference between the crystal and undercooled liquid. Kauzmann pointed out[14] that in general the entropy of the liquid decreases faster than the entropy of the crystal. If this situation were to continue, the entropy of the undercooled liquid would become smaller than that of the crystal at a critical temperature T_{g0} ($= T_{\Delta S=0}$), the ideal glass transition temperature. This situation can be avoided by massive freezing of the liquid to a glass above T_{g0} (Kauzmann paradox[14]). For some pure metals this point is found at about 0.25 of the melting temperature.[15] For the glass-forming alloy $Au_{53.2}Pb_{27.5}Sb_{19.3}$ the ideal glass transition temperature, where S^L equals S^x, is found at 313 ± 5 K (within the error range of the C_p measurement). This corresponds to 0.55 of the liquidus temperature T_L (reduced glass transition temperature) and gives the maximum undercooling limit of the liquid phase. This temperature agrees well with the experimentally observed glass transition temperature by heating a Au-Pb-Sb glass through T_g.[5] The fact that S^L equals S^x at T_{g0} reflects the rapidity with which entropy is removed with decreasing temperature. The unlikely circumstance that the entropy difference between the undercooled liquid and crystal becomes negative below a nonzero temperature indicates an "entropy crisis" as the stability limit for the undercooled liquid. The actual temperature of the glass transition which is purely kinetic in origin, occurs at slightly higher temperature at finite entropy difference leaving an excess entropy in the glass.

In general, the divergence between T_{g0} (ideal) and T_g (actual) reflects the degree of departure from internal configurational equilibrium during the vitrification of an undercooled liquid. As a result, the more rapid the quench rate involved in glass formation, the larger is the separation between T_{g0} and T_g. Therefore, it is not surprising that in the present case there is only a small $T_{g0} - T_g$ difference since the AuPbSb glasses are expected to be in a well relaxed configurational state.

Downloaded 12 Jan 2006 to 131.215.240.9. Redistribution subject to AIP license or copyright, see http://jap.aip.org/jap/copyright.jsp

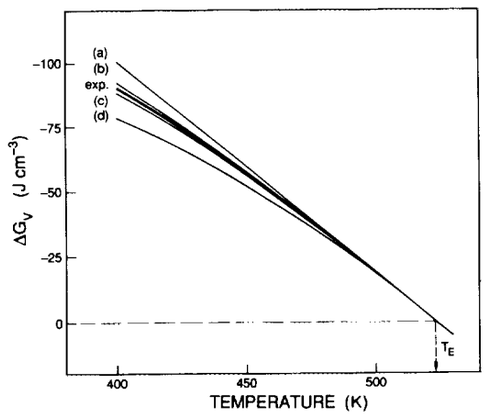

FIG. 7. Free-energy difference between undercooled liquid and eutectic solid per unit volume based on different approximations including the experimental data. Curves (a)–(d) refer to Eqs. (9a)–(9d), respectively.

TABLE I. Analysis of nucleation kinetics according to classical nucleation theory [Eqs. (3) and (5)] and different models for the Gibbs free-energy difference ΔG_V per unit volume. In addition, the Kauzmann temperature $T_{\Delta S=0}$ is given for the different ΔG_V models.

ΔG_V (J/cm^3)	$T_{\Delta S=0}$ (K)	A (s^{-1})	B (K J^2 cm^{-6})
Experimental	313	1.8×10^{16}	1.02×10^{8}
Ref. 16	$-\infty$	2.4×10^{13}	1.03×10^{8}
Ref. 17	209	2.1×10^{15}	0.99×10^{8}
Ref. 18	216	1.2×10^{16}	0.97×10^{8}
Ref. 19	261	1.1×10^{19}	0.93×10^{8}

An important parameter in the analysis of the kinetics of crystallization at high undercooling is the Gibbs free-energy difference between metastable liquid and crystalline solid ΔG_V and its dependence on temperature. From Eqs. (6) to (8) it is seen that ΔG_V is primarily a function of the heat capacity difference $\Delta C_p(T)$ between undercooled liquid and crystalline solid which is unknown in most cases. Therefore, different models have been proposed for ΔG_V using such easily accessible data as the heat of fusion ΔH_f, the heat capacity difference ΔC_p^f at the melting or eutectic temperature, and the undercooling level $\Delta T = T_E - T$ below the eutectic temperature T_E or melting point. Several approaches for crystallization of a single solid phase are given below such as

$$\Delta G_V = \Delta H_f \Delta T / T_E \quad \text{(Ref. 16)}, \tag{9a}$$

$$\Delta G_V = \Delta H_f \Delta T / T_E - [\Delta C_p^f (\Delta T)^2 (1 - \Delta T/6T)]/2T \quad \text{(Ref. 17)}, \tag{9b}$$

$$\Delta G_V = \Delta H_f \Delta T\, 2T/[T_E(T_E + T)] \quad \text{(Ref. 18)}, \tag{9c}$$

$$\Delta G_V = \Delta H_f \Delta T\, T/(T_E)^2 \quad \text{(Ref. 19)}. \tag{9d}$$

Figure 7 presents different approximations proposed for the free-energy difference ΔG_V between undercooled liquid and eutectic solid including the experimentally derived values. It is seen from Fig. 7 that at low undercooling all formulas predict basically the same ΔG_V in excellent agreement with the experimental curve. At modest undercooling the best correlation between experimental data and the proposed models over the measured temperature range are obtained with Eq. (9b) (Ref. 17) and Eq. (9c).[18] As has been found earlier, Turnbull's approximation [Eq. (9a)] gives an upper limit for ΔG_V and is close to values obtained for pure metals,[13] whereas Hoffman's expression underestimates ΔG_V in the case of glass-forming metallic alloys.[20] In addition, the Kauzmann temperatures $T_{\Delta S=0}$ where $-\partial \Delta G_V/\partial T$ equals 0, are estimated for the given models in Eqs. (9a)–(9d) and are given in Table I. They are all lower than the Kauzmann temperature extrapolated from the measurement and differ considerably for the different models ranging from $-\infty$ [Eq. (9a) (Ref. 16)] to 261 K [Eq. (9d) (Ref. 19)].

One consequence of the correct evaluation of ΔG_V relates to the proper interpretation of crystallization kinetics.[9] The measured prefactor term A is in good agreement with the classical nucleation theory for heterogeneous nucleation [$\Omega_a = \sim 10^{23}$ cm^{-3} s^{-1} (Refs. 7 and 8)] if only a small portion (10^{-3}) of the surface area presents an active catalytic site for crystallization. Using the same type of analysis as outlined above [Eq. (5)] for the experimentally derived nucleation data and basing ΔG_V on Eqs. (9a)–(9d) would lead to a difference in the prefactor term A in the nucleation rate expression of several orders of magnitude as given in Table I. Whereas ΔG_V differs only about 20% at 420 K for the different models, the derived constants A can vary by six orders of magnitude ranging from $A = 2.4\times10^{13}$ s^{-1} [Eq. (9a)] to 1.1×10^{19} s^{-1} [Eq. (9d)] in comparison to 1.8×10^{16} s^{-1} for the experimentally derived value. In comparison, the slope B shows only a small dependence on the model with a variation of less than 10%.

Based upon the fit of experimental data in Fig. 6 it is possible to develop the complete transformation diagram that is described by Eq. (8). If the parameters A and B are treated as approximately constant with temperature, curve (a) in Fig. 8 is obtained. While all these calculations are approximate due to estimates of some of the parameters and the limited temperature range of the experimental data, the results do offer an interesting viewpoint on the kinetics. With the use of different model approximations for the Gibbs free energy of crystallization ΔG_V the nucleation frequencies should be properly corrected in terms of the prefactor obtained for each model which can vary about six orders of magnitude. To illustrate this in more detail, the curves as obtained on the basis of the different model approximations for ΔG_V [Eqs. (9a)–(9d)] and the corresponding parameters A and B (Table I) are included in Fig. 8 as curves (a)–(d). The cooling rates necessary to avoid crystallization differ by a factor of 10^4 between the experimental values and the data based on the different models with the linear approximation requiring the highest cooling rate. But none of these

Downloaded 12 Jan 2006 to 131.215.240.9. Redistribution subject to AIP license or copyright, see http://jap.aip.org/jap/copyright.jsp

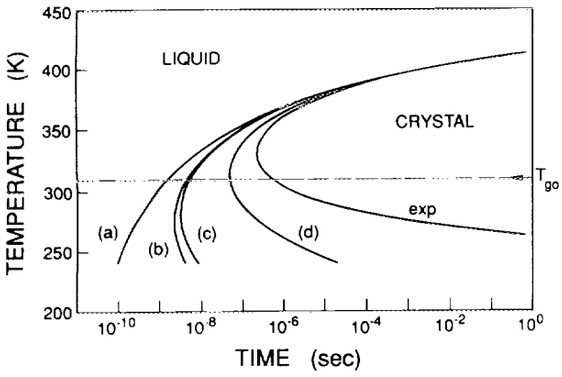

FIG. 8. Calculated steady-state heterogeneous nucleation kinetics of $Au_{x_2}Pb_{y_2}Sb_{z_2}$ droplets samples based on Eq. (5) for different approximations for ΔG_v with the prefactor A taken as temperature independent and the experimentally derived ideal glass transition temperature indicated as T_{g0}. In addition to the curve extrapolated on the basis of experimental data (exp.), curve (a) represents the approximation by Turnbull and Fisher (Ref. 16), (b) Dubey and Ramachandrarao (Ref. 17), (c) Thompson and Spaepen (Ref. 18), and (d) Hoffman (Ref. 19), respectively.

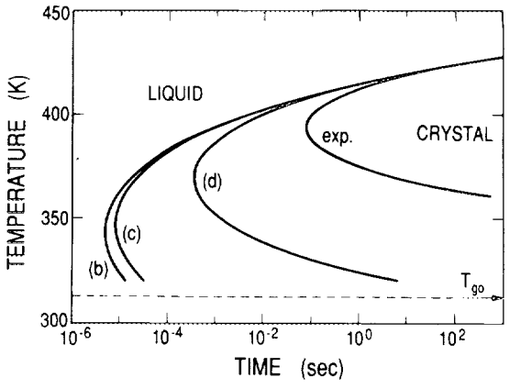

FIG. 9. Calculated steady-state heterogeneous nucleation kinetics of glass-forming Au-Pb-Sb alloys based on Eq. (5) including a correction for the temperature dependence of the viscosity of the prefactor terms $A(T)$ for the different models for ΔG_v and the resulting ideal glass transition temperatures as given in Table I with the experimentally derived ideal glass transition temperature indicated as T_{g0}. The curves correspond to the extrapolation of experimental data (exp.), (b) to the approximation of ΔG_v and $T_{\Delta S=0}$ by Dubey and Ramachandrarao (Ref. 17), (c) by Thompson and Spaepen (Ref. 18), and (d) by Hoffman (Ref. 19), respectively.

calculated curves agree with the observation that a critical cooling rate of $\sim 10^5$ K/s, as obtained in drop tubes, is sufficient to form a glass.

In the more realistic case, especially important for glass-forming alloys, the temperature dependence of the prefactor term A, i.e., the viscosity change of the undercooled liquid as function of undercooling should be taken into account. This can be done by appropriately correcting the factor $A = a\Omega_a/[K(T_N)\eta]$. Based on the above evaluation, the prefactor terms are determined in a narrow range of the nucleation temperatures. Using Eq. (3a) as model for the temperature dependence of the viscosity $\eta(T)$, which agrees with measured data at higher temperatures measured around 870 K,[21] a modified prefactor term is used as $A(T) = A\eta(T_N)/\eta(T)$.

With this correction for the temperature dependence of the viscosity, the TTT curves of Fig. 8 have been recalculated with the extrapolated Kauzmann temperatures from Eqs. (9) taken as critical temperature for the viscosity [Eq. (3a)]. Whereas a linear approximation for ΔG_v is not applicable for glass-forming alloys ($T_{g0} = -\infty$), all other approximations[17–19] depict the "nose" of the transformation curve at considerably shorter times than in Fig. 8. For the various approximations the "noses" of the TTT curves are obtained at 8×10^{-2} s and 393 K (exp), 5×10^{6} s and 343 K [Ref. 17, curve (b)], 8×10^{6} s and 343 K [Ref. 18, curve (c)], and 3×10^{-4} s and 369 K [Ref. 19, curve (d)], as shown in Fig. 9. According to this analysis, higher cooling

TABLE II. The position of the "noses" of the TTT curves [t(s)/T(K)] from Eq. (5). Different approaches for the location of the T_{g0} temperature describing the temperature dependence of the viscosity [Eq. (3a)] and the parameters for A and B as derived from the C_p measurements (exp) or from theoretical models according to Refs. 16–19 have been used.

T_{g0}	Parameters A and B as given in Table I				
(K)	Exp.	a	b	c	d
313[a,b]	8×10^{-2}/393	6×10^{-3}/392	6×10^{-2}/392	6×10^{-2}/392	7×10^{-2}/393
$-\infty$[c]	...	...	...	...	...
209[b]	2×10^{5}/355	3×10^{6}/339	5×10^{6}/343	5×10^{6}/344	1×10^{5}/351
216[c]	3×10^{5}/357	5×10^{6}/342	8×10^{6}/346	8×10^{6}/343	2×10^{5}/353
261[d]	5×10^{-4}/371	2×10^{-4}/365	2×10^{-4}/365	2×10^{-4}/366	3×10^{-4}/369

[a] See Ref. 16.
[b] See Ref. 17.
[c] See Ref. 18.
[d] See Ref. 19.

Downloaded 12 Jan 2006 to 131.215.240.9. Redistribution subject to AIP license or copyright, see http://jap.aip.org/jap/copyright.jsp

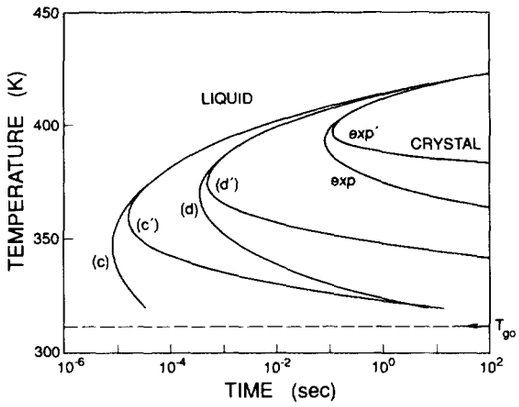

FIG. 10. Difference between steady-state heterogeneous nucleation kinetics and nucleation kinetics including transient nucleation effects with the experimentally derived ideal glass transition temperature indicated as T_{go}. The three curves (exp), (c), and (d) from Fig. 9 (steady state) are redrawn and shown in comparison to curves (exp'), (c'), and (d') including transient nucleation effects.

rates would be required for curves (b), (c), and (d) to avoid crystallization than the experimentally determined critical rate of about 10^3 K/s.[5] The only curve, consistent with the experimental observation that crystallization is avoided at cooling rates of $\sim 10^3$ K/s, is represented by the curve (exp) which is based on the measured data. Consequently, the ΔG_V models as given by Eqs. (9a)–(9d) are inappropriate in order to analyze the crystallization kinetics of glass-forming Au-Pb-Sb alloys at large undercooling taking the Kauzmann temperature as the critical temperature for the temperature dependence of the viscosity.

Moreover, it should be mentioned that the analysis as outlined above is only valid for steady-state conditions. For many situations, especially for nucleation at large undercooling, transient nucleation effects in some alloy systems are not negligible.[22] Within this approach, the time dependence of the nucleation frequency may be estimated approximately by

$$J(T,t) = J_a(T)\exp[-\tau(T)/t], \tag{10}$$

where the transient time $\tau(T)$ is given by

$$\tau(T) = 3\pi^2 d^3 \eta / k_B T, \tag{11}$$

with d being a characteristic length taken to be the average atomic diameter (~ 4 Å) for use with the Stokes–Einstein relation.[22] As noted by Kelton *et al.*,[22,23] a more accurate accounting of transient effects is possible, but would involve additional uncertainties on nucleus formation in the present case where vitrification is competing with eutectic crystallization. From the estimates in Eqs. (10) and (11) the transient effects appear to become important at temperatures below 400 K for this alloy system. As a consequence, the steady-state transformation curves as depicted in Fig. 9 are shifted to slightly shorter times if transient effects are taken into account. This is shown in Fig. 10 exhibiting the steady-state kinetics curves (exp), (c) and (d), and comparing them to the curves corrected for transient nucleation effects (exp'), (c') and (d'). [Curve (b) is not shown because it is very similar to curve (c).] It is seen that the shifts of the curves are very pronounced for large undercooling but the "noses" are only slightly shifted to shorter times. The analysis demonstrates that transient nucleation effects are important at high undercooling, but do not affect the critical cooling rate to avoid crystallization in Au-Pb-Sb alloys considerably. It is interesting to note that the minor influence of non-steady-state conditions on glass-forming Au-Pb-Sb alloys is in accord with the analysis by Kelton *et al.*[22] Therefore, only the measured curve (exp) agrees with the experimental observation that crystallization can be avoided at cooling rates of $\sim 10^3$ K/s, whereas all other approximations fail for this condition.

The experiments which have been done for modest undercooling ($\sim 27\%\ T_L$) indicate the difficulties to extrapolate the thermodynamic functions of the Gibbs free energy and the related entropy difference into the glass-forming regime and the impact of these difficulties on the assessment of crystallization kinetics. It is obvious that transient nucleation and, in particular, viscosity effects are becoming important below 400 K, i.e., at about 0.3 T_L undercooling. Whereas for the crystallization kinetics of pure metals both of these effects are almost negligible, they become very pronounced for glass-forming alloys. However, due to the use of the Stokes–Einstein relation to estimate the diffusivity, the influence of the viscosity and transient nucleation effects on the nucleation rates are strongly coupled. Because diffusivity data are unknown in the highly undercooled liquid state, it is usually very difficult to separate the two effects.

Due to limitations in the theory for the glass transition[24,25] and the lack of many dynamical properties of highly undercooled liquids including the viscosity η, diffusion coefficients D, and resulting transient times τ, the correct description of the crystallization kinetics in the highly undercooled regime and/or glass formation can therefore not be reduced simply to the application of existing models for the free-energy difference ΔG_V and viscosity. Based on the current work a reasonable assessment of the competition between glass formation and crystallization over a wide range of undercooling and cooling rate is possible if experimental data for the nucleation rates and thermodynamic data for the free-energy functions as obtained at low and modest undercooling are available. This reveals the importance of using measured values of thermophysical properties for extrapolations into the glass-forming regime, even if the measurements represent a limited temperature range, in comparison to model approximations that are often inconsistent and only valid at low undercooling. However, the present results do not rule out the possibility of a phase separation reaction which has been found in Au-Pb-Sb glasses,[2] but further studies, which are in progress, are required to examine this feature.

ACKNOWLEDGMENTS

Fruitful discussions with Professor D. Turnbull, Professor P. Haasen, and Dr. K. Ohsaka and the financial support from NASA (NAS 496954MG3203550, NAG-8-771) and ARO (DAAL 03-90-G-0042) are gratefully acknowledged.

Downloaded 12 Jan 2006 to 131.215.240.9. Redistribution subject to AIP license or copyright, see http://jap.aip.org/jap/copyright.jsp

[1] C. O. Kim and W. L. Johnson, Phys. Rev. B **23**, 143 (1981).
[2] M. C. Lee, J. M. Kendall, and W. L. Johnson, Appl. Phys. Lett. **40**, 382 (1982).
[3] J. H. Perepezko and J. S. Paik, Mater. Res. Soc. Symp. Proc. **8**, 49 (1982).
[4] J. H. Perepezko and J. S. Smith, J. Non-Cryst. Solids **44**, 65 (1981).
[5] M. C. Lee, H. J. Fecht, J. L. Allen, J. H. Perepezko, K. Ohsaka, and W. L. Johnson, J. Mater. Sci. Eng. **97**, 301 (1988).
[6] R. Becker and W. Döring, Ann. Phys. **24**, 719 (1935).
[7] D. Turnbull, J. Chem. Phys. **20**, 411 (1952).
[8] C. V. Thompson and F. Spaepen, Acta Metall. **31**, 2021 (1983).
[9] J. H. Perepezko, B. A. Mueller, and K. Ohsaka, *Hume-Rothery Memorial Symposium on Undercooled Alloy Phases*, edited by E. W. Collings and C. C. Koch (The Metallurgical Society, New Orleans, LA, 1986), p. 289.
[10] J. H. Perepezko and Rasmussen, Met. Trans. A **9**, 1490 (1978).
[11] H. S. Chen and D. Turnbull, J. Appl. Phys. **38**, 3646 (1967).
[12] H. W. Kui and D. Turnbull, J. Non-Cryst. Solids **94**, 62 (1987).
[13] J. H. Perepezko and J. S. Paik, J. Non-Cryst. Solids **61&62**, 113 (1984).
[14] W. Kauzmann, Chem. Rev. **43**, 219 (1948).
[15] H. J. Fecht and W. L. Johnson, Nature **334**, 50 (1988).
[16] D. Turnbull and J. C. Fisher, J. Chem. Phys. **17**, 71 (1949).
[17] K. S. Dubey and P. Ramachandrarao, Acta Metall. **32**, 91 (1984).
[18] C. V. Thompson and F. Spaepen, Acta Metall. **27**, 1855 (1979).
[19] J. D. Hoffman, J. Chem. Phys. **29**, 1192 (1958).
[20] L. Battezzati and L. Garrone, Z. Metallkd. **75**, 305 (1984).
[21] A. E. Lord, Jr. and J. Steinberg, J. Appl. Phys. **54**, 6038 (1983).
[22] K. F. Kelton and A. L. Greer, J. Non-Cryst. Solids **79**, 295 (1986).
[23] K. F. Kelton, A. L. Greer, and C. V. Thompson, J. Chem. Phys. **79**, 6261 (1983).
[24] P. W. Anderson, in *Ill Condensed Matter*, edited by R. Balian, R. Maynard, and G. Toulouse (North-Holland, Amsterdam, 1979), p. 159.
[25] N. O. Birge and S. R. Nagel, Phys. Rev. Lett. **54**, 2674 (1985).

Downloaded 12 Jan 2006 to 131.215.240.9. Redistribution subject to AIP license or copyright, see http://jap.aip.org/jap/copyright.jsp